ASSESSMENT OF AN INTEGRATED SOLAR COMBINED CYCLE SYSTEM BASED ON CONVENTIONAL AND ADVANCED EXERGETIC METHODS

by

Shucheng WANG[a], Pengcheng WEI[a], Sajid SAJID[b], Lei QI[a], and Mei QIN[a*]

[a] School of Energy Power and Engineering,
Northeast China Electric Power University, Jilin, China
[b] State Key Laboratory of Alternate Electrical Power,
System with Renewable Energy Sources, School of Renewable Energy,
North China Electric Power University, Beijing, China

Original scientific paper
https://doi.org/10.2298/TSCI210825325W

An integrated solar combined cycle system based on parabolic trough solar collector and combined cycle power plant is proposed. The advanced system is socio-economic significance compared to traditional combined cycle power system. Plainly, the exergetic analyses (exergy destruction and efficiency) via conventional and advanced methods are used for thermodynamic properties of the integrated solar combined cycle system components. In addition, the exergy destruction is divided into endogenous, exogenous, avoidable, and unavoidable. The results show that the combustion chamber has the largest fuel exergy and the highest endogenous exergy destruction rate of 1001.60 MW and 213.87 MW, respectively. Additionally, the combustion chamber has the highest exergy destruction rate of 235.60 MW (60.29%), followed by the parabolic trough solar collector of 54.20 MW (13.87%). For overall system, the endogenous exergy destruction rate of 320.83 MW (82.10%) and exogenous exergy destruction rate of 69.97 MW (17.90%) are resulted via the advanced exergy analysis method. Besides, Several methods to reduce the exergy destruction and improve the components' efficiency are put forward.

Key words: *combined cycle power plant, advanced exergetic analysis, exergy destruction, exergy efficiency*

Introduction

Parabolic trough solar collector (PTSC) technology is one of the most promising solar thermal power generation technologies [1-3]. An integrated solar combined cycle system (ISCCS) consists of a PTSC system and a combined cycle power plant (CCPP) system. However, the challenge is to reduce the cost of this technology compared with traditional power generation systems [4]. The ISCCS can provide significant solar integration allotment into the system, achieve substantial economic and environmental friendliness compared to solar integration into other types of power cycles [5]. The net thermal efficiency of the ISCCS plant has been demonstrated over 60% which is 5~10% higher than the conventional CCPP systems [6]. In addition, natural gas is a source of clean energy, less pollutant emitter and an alternative for environmental protection [4, 7]. The ISCCS has been widely recognized for its superior environmental protection performance, high thermal efficiency, energy saving, water saving,

* Corresponding author, e-mail: mq@neepu.edu.cn

load stability and other advantages of interest implemented in different regions of the world [8]. The energy utilization efficiency, energy conversion and components destruction of a system can be analyzed through exergetic analyses method. Baghernejad *et al.* [9] has been analyzed the ISCCS using the energy and exergy analysis method to investigate the plant performance and pinpoint sites of primary exergy destruction. It has been noticed that the energy and exergy efficiencies values for ISCCS were higher than simple CCPP. Thermal power systems driven by PTSC with detailed exergy analysis method has also been displayed higher energy efficiency with increased solar radiation.

However, the conventional analysis does not take into account the components' interaction and real potential for energy conversion improvement in the complex system [10]. To overcome this shortcoming an advanced exergetic analysis method has been reported [11]. The bottom ORC cycle via conventional and advanced exergetic analysis has been displayed high potential improvement [12]. Besides, the advanced exergetic analysis revealed expander as the first improvement priority followed by pump, condenser and boiler. In addition, the advanced exergetic analysis has been shown the endogenous/exogenous irreversibilities and combination with avoidable/unavoidable irreversibilities of each component for real CCPP [13]. The avoidable exergy destruction rate has been affected by 20.7% with an increased compressor pressure ratio for the combustion chamber. Furthermore, a diagnosis method based on advanced exergetic analysis has been studied for coal-fired power plants. Strikingly, this method has been identified the deviations successfully [14]. Noticeably, the advanced exergetic analysis method has a key role to analyze exergy destruction of complex system components especially in the investigation of ISCCS. Song *et al.* [15] determined the solid oxide fuel cell system combined with a kinetic-based molding pre-reformer using conventional and advanced analysis. The results showed that the component heat exchanger is the greatest potential for improvement due to the largest avoidable endogenous exergy destructions and negative endogenous destructions. Yang *et al.* [16] performed the advanced exergy analysis to achieve more valuable information by taking the component interconnections and technological limitations. The results indicated that the interactions among components are weak and the proposed system had a large potential for improvement due to the avoidable exergy destruction. Li *et al.* [17] provide directions for further improvement on the efficiency of this system and deeper understandings of interactions between the components for the proposed system via the conventional and the advanced exergy analysis methods. Zhang *et al.* [18] analyzed an integrated energy storage system based on transcritical CO_2 energy storage and ORC via the conventional and advanced exergy analyses. Results showed that the proposed system had great potential for the improvement of system performance for the exergy efficiency was 34.62% under the real condition and the theoretical maximum for unavoidable condition was 43.48%. Wang *et al.* [19] proposed a system integrated the CO_2 capture and storage process and the waste heat utilization processes. It results provided guidance for the optimization of system irreversibility and help to determine the improvement potential of components. Jain *et al.* [20] reported the thermodynamic potential and risk estimation of NH_3-H_2O and H_2O-LiBr integrated vapor absorption refrigeration system via the advanced exergy analysis.

Herein, the assessments of the overall design of ISCCS to reduce exergy destruction and improve exergy efficiency are analyzed. The highest and main exergy destruction is pointed out in the combustion chamber and PTSC. Besides, the main exergy destruction is divided into endogenous, exogenous, avoidable, and unavoidable. Compare to other research using advanced exergy analysis method, our results firstly provide the significance of the applied exergetic analysis method to reduce exergy destruction and improve energy-saving in ISCCS.

System description

The model is built on a conventional CCPP system (SGT5-4000F), which includes a SIEMENS V94.3A gas turbine and a three-pressure HRSG with reheat. As depicted in fig. 1, a part of compressed air is used to cool turbine blades while the remaining is burned with natural gas in the combustion chambers. The expanded exhaust gas with high temperature and pressure in turbines operates a generator to produce electricity. Furthermore, the flue gas gets into HRSG and heats the supplied steam. The HRSG has three different pressure levels such as HP, IP, and LP with economizers, evaporators, and superheaters. Firstly, the economizer heats water and then supplies it to the evaporator to get saturated steam. Secondly, the produced superheated steam at three different pressures and temperatures is injected into steam turbines.

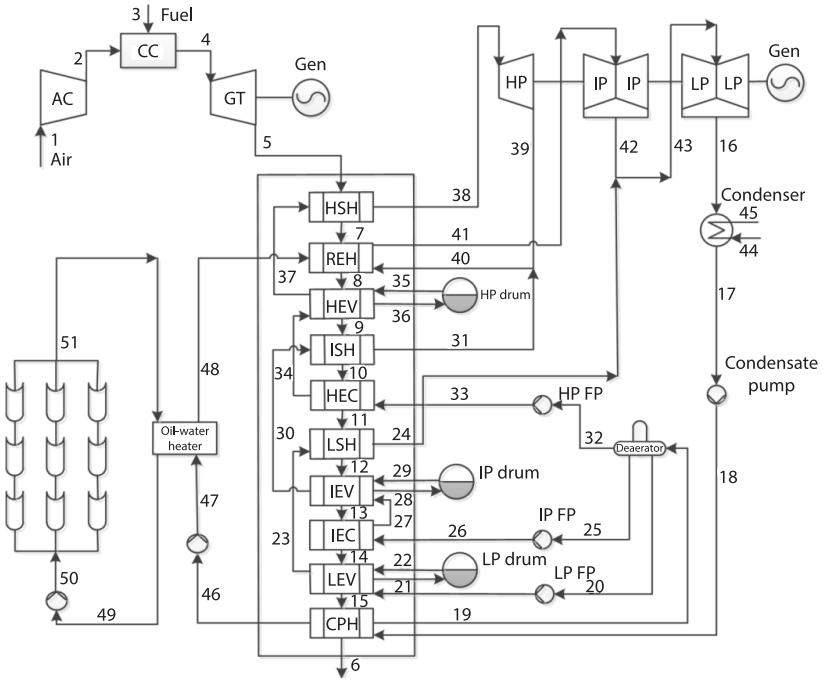

Figure 1.

The PTSC is coupled to the conventional CCPP. A part of feed water (149 °C) from the condensate preheater is injected into the heat exchanger of PTSC and heated to superheated steam (358 °C). Then it is mixed with the exhaust steam (351°C) of the high pressure turbine and the intermediate pressure superheated steam (329.5 °C). The reheater further heats these steams to the temperature of 349 °C before they are injected back to the intermediate pressure turbine.

Mathematical modelling

Energy and conventional exergy analysis

The thermodynamic balance of the ISCCS is defined [13]:

$$\dot{Q} + \sum \dot{m}_{\text{in}} h_{\text{in}} = \dot{W} + \sum \dot{m}_{\text{out}} h_{\text{out}} \tag{1}$$

$$Q_{\text{u}} = \dot{m}(h_{\text{out}} - h_{\text{in}}) \tag{2}$$

where $\dot{Q}$ and $\dot{W}$ are entering the energy and output work of a system. Similarly, the expressions for combustion reactions [21, 22]:

$$\begin{aligned}\lambda \mathrm{C}_{x_1}\mathrm{H}_{y_1} + (x_{\mathrm{O}_2}\mathrm{O}_2 + x_{\mathrm{N}_2}\mathrm{N}_2 + x_{\mathrm{H_2O}}\mathrm{H_2O} + x_{\mathrm{CO}_2}\mathrm{CO}_2 + x_{\mathrm{Ar}}\mathrm{Ar}) \\ \rightarrow y_{\mathrm{CO}_2}\mathrm{CO}_2 + y_{\mathrm{N}_2}\mathrm{N}_2 + y_{\mathrm{H_2O}}\mathrm{H_2O} + y_{\mathrm{Ar}}\mathrm{Ar} \\ y_{\mathrm{CO}_2} = (\lambda x_1 + x_{\mathrm{CO}_2}), \quad y_{\mathrm{N}_2} = x_{\mathrm{N}_2} \\ y_{\mathrm{H_2O}} = \left(x_{\mathrm{H}_2 O} + \frac{\lambda y_1}{4}\right), \quad y_{\mathrm{Ar}} = x_{\mathrm{Ar}}, \quad \lambda = \frac{n_{\mathrm{f}}}{n_{\mathrm{air}}}\end{aligned} \tag{3}$$

The mole values of flue gas can be calculated by the aforementioned formula and λ are the mole ratio of the fuel to air mixture.

For collector system, the amount of solar thermal energy available depends on the total area of collectors and direct normal irradiation (DNI) [23]:

$$Q_{\mathrm{i}} = N \times A \times DNI \tag{4}$$

where N is the number of collectors and A – the area of collectors. The energy absorbed by the absorber tube was given:

$$Q_{\mathrm{r}} = \eta Q_{\mathrm{i}} \tag{5}$$

where η is the optical efficiency of the collectors which depends on the surface reflectivity of compound parabolic concentrator (CPC), receiver transmissivity, receiver absorption rate, acquisition factor, mirror utilization rate, radiation, convective heat loss efficiency, and a correction factor of the incident angle. Furthermore, the η is expressed:

$$\eta = \eta_\rho \eta_\tau \eta_\alpha \eta_\gamma \eta_\phi \eta_\mu K \tag{6}$$

where η_ρ is the surface reflectivity of CPC, η_τ – the receiver transmissivity, η_α – the receiver absorption rate, η_γ – the acquisition factor, η_ϕ – the mirror utilization rate, η_μ – the radiation and convective heat loss efficiency, and K – the correction factor of incident angle.

According to the balance conventional exergy analysis, the exergy is the part of the energy that cannot be completely converted to mechanical energy. Stream exergy consists of physical exergy and chemical exergy when potential and kinetic exergies are neglected [22]:

$$\dot{E}x = \dot{E}x_{\mathrm{ph}} + \dot{E}x_{\mathrm{ch}} \tag{7}$$

where physical and chemical exergies are defined as [21, 22, 24]:

$$\dot{E}x_{\mathrm{ph}} = \dot{m}\left[(h - h_0 - T_0(s - s_0)\right] \tag{8}$$

$$\dot{E}x_{\mathrm{ch}} = \dot{m}\left[\sum_{i=1}^{n} x_i Ex + \mathrm{R}T_0 \sum_{i=1}^{n} x_i \ln x_i\right] \tag{9}$$

It is complicated to calculate the chemical exergy of fuels with the previous equation. Therefore, the following equation is used for the calculation [25]:

$$\dot{E}x_{\mathrm{f}} = \xi LHV_{\mathrm{f}} \tag{10}$$

where LHV is the lower heating value of natural gas and ξ – the the ratio of fuel chemical exergy to a low calorific value of 1.06.

The exergy of solar radiation absorbed by the receiver tube can be calculated by Petela's formula which is expressed [26]:

$$Ex_{\mathrm{a}} = Q_{\mathrm{s}}\psi \tag{11}$$

where for the ideal process, Q_s is the received solar energy. The stands for the maximum work obtained from the solar radiation [27, 28]:

$$\psi = 1 - \frac{4}{3}\frac{T_0}{T_s} + \frac{1}{3}\left(\frac{T_0}{T_s}\right)^4 \tag{12}$$

where T_0 and T_s are the ambition temperature and the equivalent temperature of the Sun as a black body (~5770 K), , respectively.

Advanced exergetic analysis

The primary method for the implementation of the advanced exergy analysis is the conventional exergy analysis method. The comparative results of two kinds of analysis can calculate the exergy destruction due to the low efficiency of each component. The processing system and thermodynamic system always pay a certain price to achieve a certain product. The cost is defined as *fuel* and the final yield is called *product*. Furthermore, *fuel* and *products* refer to the exergy input and output of a subsystem. The difference between fuel exergy consumed $\dot{E}x_{F,k}$ and product exergy $\dot{E}x_{P,k}$ is expressed as exergy destruction $\dot{E}x_{D,k}$ in the process of energy conversion [29]:

$$\dot{E}x_{D,k} = \dot{E}x_{F,k} - \dot{E}x_{P,k} \tag{13}$$

Exergy efficiency and the destruction rate of k^{th} component are defined [23]:

$$\varepsilon_k = \frac{\dot{E}x_{P,k}}{\dot{E}x_{F,k}} \tag{14}$$

$$y_{D,k} = \frac{\dot{E}_{D,k}}{\dot{E}_{F,k}} \tag{15}$$

For the overall system, the exergy balance equation can be written [30]:

$$\dot{E}_{F,tot} = \dot{E}_{P,tot} + \sum_k \dot{E}_{D,k} + \dot{E}_{L,tot} \tag{16}$$

where $\dot{E}x_{F,tot}$ is the fuel exergy entering to the system, $\dot{E}x_{P,tot}$ – the product exergy, and $\dot{E}x_{L,tot}$ – the exergy lost in the system (the heat loss from smoke evacuation or leaking of the system).

There is no doubt that every component interacts with each other in a complex system. It is obvious that the variable working state of a component leads to change thermodynamic properties. In order to analyze the interaction between components, exergy destruction is divided into endogenous and exogenous exergy destruction [30-34]:

$$\dot{E}x_{D,k} = \dot{E}x_{D,k}^{EN} + \dot{E}x_{D,k}^{EX} \tag{17}$$

For the potential energy saving of system components, the advanced exergy analysis method of exergy destruction is categorized as avoidable and unavoidable [30-35]:

$$\dot{E}x_{D,k} = \dot{E}x_{D,k}^{AV} + \dot{E}x_{D,k}^{UN} \tag{18}$$

Assumptions and system parameters

Assumptions

The considerations are followed in various operating conditions during the analysis as [13, 25]:

– All processes are steady-state along with constant DNI.

– The temperature and mass-flow rate are constant for the exhaust gases from the gas turbine.
– The fuel is natural gas at a lower heating value (LHV = 49015 kJ/kg).
– The ambient operating temperature and pressure are 20 ℃ and 1.0 bar, respectively.

System parameters

The viable mathematical model of the PTSC system and a CCPP are built by EBSILON® Professional, which is widely used in power plant design, evaluation, optimization, and other thermal cycle processes. In order to validate the accuracy of the simulation process of the proposed model, a series of main parameters were selected. The design values and simulation results with an acceptable range of relative error in main parameters are shown in tab. 1. Thermal systems, mainly analyze through two approaches: one is based on the First law of thermodynamics (the energy and conventional exergy analysis) while the other is based on the First and the Second law of thermodynamics (the advanced exergy analysis). Importantly, the exergy analysis method reveals the cause, location, and direction of the destruction compared to energy analysis.

Table 1. Main parameters of SGT5-4000F

Parameters	Design values	Simulation results	Units
Capacity	387	389	[MW]
Main steam	12.5/566/72.6	12.6/567/73.1	[MP], [°C], [kgs^{-1}]
Reheated steam	2.99/551/85.6	2.91/551/87.8	[MPa], [°C], [kgs^{-1}]
Low pressure steam	0.45/239/12.3	0.46/240/12.9	[MPa], [°C], [kgs^{-1}]
Gas turbine exhaust	590/643	590.6/646	[°C], [kgs^{-1}]
Ambient temperature	20	20	[°C]
Exhaust gas temperature	90	90.9	[°C]

The parameters of CCPP are based on the SGT5-4000F running data from an Electric Power Generation. The thermal performance of PTSC is collected from Salgado *et al.* [32]. This plant is located at 113°42′E, 34°44′N, with 57% peak optical efficiency of PTSC. The ambient temperature is 20 °C, wind speed is 1.5 m/s and the DNI is about 800 W/m^2. The aforementioned analysis is carried out on the 2st of June at 12:00 a. m. The estimation of unavoidable conditions is assumed from previously reported work [13] and the basic parameters are shown in tab. 2. The endogenous exergy destruction is related to the operation of component k it self. It is obtained when the considered component operates under real conditions and all other components of the process operate without irreversibility (theoretically) [10].

Table 2. The basic parameters for advanced exergetic analysis

Component, k	Real condition	Theoretical condition	Unavoidable condition
Compressor	η_{th} = 98%	η_{th} = 100%	η_{th} = 99%
CC	Q_L = 2%	Q_L = 0%	Q_L = 0%
Expanders	η_{th} = 98%	η_{th} = 100%	η_{th} = 99%
Exchangers	ΔP_{12} = 0.05 Pa	ΔP_{12} = 0 Pa	ΔP_{12} = 0.05 Pa
	ΔP_{34} = 0.002 Pa	ΔP_{34} = 0 Pa	ΔP_{34} = 0.002 Pa
Pumps	η_{th} = 95%	η_{th} = 100%	η_{th} = 99%
	η_{is} = 80%	η_{is} = 8100%	η_{is} = 99%

Herein, the total incident radiation on the collectors is about 183 MW with total energy absorption of 99.72 MW. The mass-flow rate of molten salt in collectors is 229.57 kg/s. The temperature of the feedwater is 149.5 °C and the outlet temperature of the superheated steam is 358.5 °C. The main design parameters of CCPP and PTSC are listed in tabs. 1 and 3.

Table 3. Main parameters of PTSC system

Parameters	Values [3, 9, 36]	Units
DNI	800	[Wm^{-2}]
Length	150	[m]
Width	5.76	[m]
Temperature of water in/out of the receiver	149.5/358.5	[°C]
Number of collectors	280	–
POEC	0.57	–
Surface reflectivity, η_ρ	0.92	–
Receiver transmissivity, η_τ	0.90	–
Receiver absorption, η_α	0.91	–
Acquisition factor , η_γ	0.93	–
Mirror utilization, η_ϕ	0.91	–
Radiation and convective heat loss efficiency, η_μ	0.90	–

Results and discussion

The thermodynamic data for each selected material stream of the overall proposed system is list in *Appendix A*. The results are used for further conventional exergetic analysis and advanced exergetic analysis.

Conventional exergetic analysis results

The conventional exergy analysis method is applied to get exergy variables for selected components as shown in tab. 4. It is revealed that the reheater, HPECON, and compressor have the highest exergy efficiency of 95.0 %, 94.87 %, and 94.37 % , respectively. The preheater displays the lowest exergy efficiency. In addition, the combustion chamber delivers the largest exergy destruction of 235.63 MW followed by PTSC of 54.21 MW and expander of 31.59 MW.

Figure 2 describes the exergy destruction and production exergy of components for the proposed system. The total value of the exergy destruction and the production exergy is the *fuel exergy*. The fuel exergy of the compressor is from the expander, the fuel exergy of the CC is from the compressed air and the fossil fuel energy. Moreover, the fuel exergy of the expander is from the work done by the exhaust gas expansion under high temperature (1247.5 °C) and pressure (1.7 MPa). It can be seen that the CC has the largest fuel exergy (1001.6 MW), followed by the expander (556.4 MW), compressor (261.7 MW), exchangers (194.4 MW), turbines (193.2 MW), solar field (99.7 MW), condenser (40.2 MW), and the deaerator (17.4 MW), while the pumps have the lowest value of 1.0 MW. Additionally, it can be noticed that the gas turbine (compressor, CC, and expander, 1819.8 MW) accounts 76.9 % of the total fuel exergy (2365.9 MW) of the overall system.

The exergy efficiency and the exergy destruction rate of selected components for the proposed system are shown in fig. 3. The deaerator has the largest exergy efficiency of 96.6%, followed by the compressor (94.37%), expander (94.32%), exchangers (90.8%), steam turbine (86.5%), and pumps (84.7%). It can be noticed that the exergy efficiency indicates the exergy

Table 4. Calculated exergy variable for selected components

Component, k	$\dot{E}_{F,k}$ [MW]	$\dot{E}_{P,k}$ [MW]	$\dot{E}_{D,k}$ [MW]	ε_k [%]	$y_{D,k}$ [%]
Compressor	261.77	247.03	14.73	94.37	5.63
CC	1001.64	766.00	235.63	76.47	23.52
Expander	556.41	524.82	31.59	94.32	5.67
Reheater	34.57	32.84	1.72	94.99	5.00
HPSH	37.57	34.31	3.25	91.33	8.66
HPEVAP	47.67	44.20	3.47	92.71	7.28
HPECON	16.86	16.00	0.86	94.87	5.12
IPSH	2.45	2.15	0.29	87.81	12.18
IPEVAP	14.44	13.53	0.91	93.67	6.32
IPECON	13.57	12.42	1.14	91.54	8.45
LPSH	1.54	1.15	0.38	74.86	25.13
LPEVAP	11.57	10.31	1.26	89.11	10.88
Preheater	14.14	9.69	4.45	68.49	31.50
HPST	28.28	26.12	2.15	92.36	7.63
IPST	69.92	58.06	11.86	83.03	16.96
LPST	95.04	83.04	12.00	87.36	12.63
HP Pump	1.03	0.87	0.15	84.81	15.18
IP Pump	0.30	0.25	0.05	82.82	17.17
LP Pump	0.001	0.001	0.0002	83.68	16.31
Condensate pump	0.07	0.06	0.01	78.04	21.95
Condenser	40.27	30.27	10.00	75.16	24.83
Deaerator	17.43	16.84	0.59	96.61	3.38
PTSC	99.72	45.51	54.20	45.64	54.35

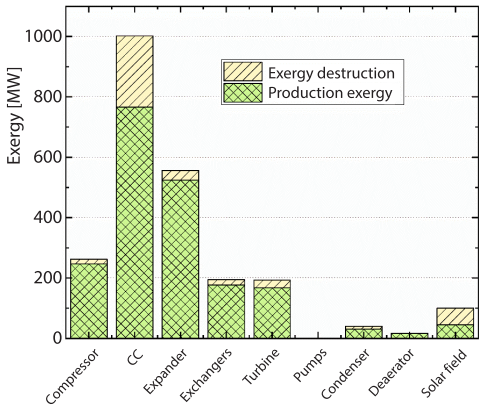

Figure 2. The exergy destruction and production exergy of components

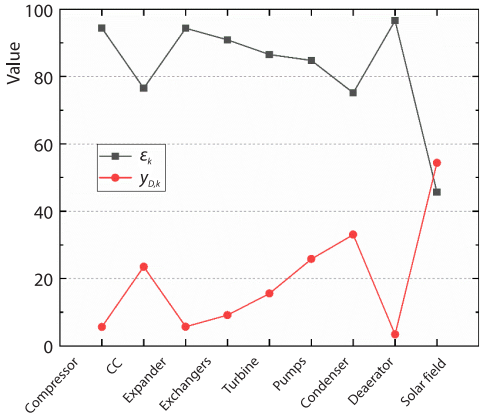

Figure 3. The exergy efficiency and the exergy destruction rate of components

utilization of the component, while the exergy destruction shows the degree of exergy loss. The solar field shows the lowest exergy efficiency of 45.6% for the reason that it has a long pipeline and a higher proportion of energy loss. Additionally, solar collectors deserve more attention improve the exergy efficiency.

Additionally, the distribution of exergy destruction for the proposed system is depicted in fig. 4. As can be seen, the CC shows the largest exergy destruction rate (235.6 MW) followed by the solar field (54.2 MW) according to the Second law of thermodynamics. For the gas turbine (compressor, CC, and expander, 282 MW), accounts for 70% of the total exergy destruction rate (390.8 MW) of the overall system. The reason why the CC has the largest exergy destruction is that the process of fuel conversion from chemical energy to the heat energy is irreversible and there is a lot of irreversible loss. In addition, the temperature of the fuel and air entering the combustion chamber is relatively low, and the temperature difference between the fuel and the exhaust gas temperature at the turbine inlet is quite large. Although the exergy efficiency of CC is relatively higher than other components from the results of fig. 3, however, the fuel exergy is quite large for the CC, which contributes to the second reason why CC has the largest exergy destruction.

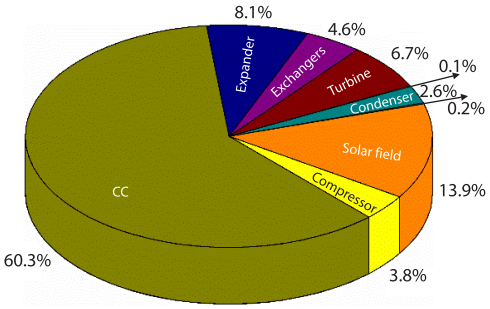

Figure 4. The distribution of exergy destruction

The exergy flow distribution of ISCCS with a solar exergy rate of 99.72 MW and natural gas exergy rate of 754.61 MW are pictured in fig. 5. A number of 415.80 MW (48.67%) of the total exergy is converted into electricity with 438.52 MW (51.33%) input loss of the system. Due to the introduction of solar collectors, the power output of the proposed ISCCS is 26.8 MW higher than the traditional combined cycle. Moreover, the fuel efficiency (55.10%) is of the overall proposed ISCCS is 3.55% higher than the conventional CCPP of 51.55%. Besides, the combustion chamber, PTSC, expander, and turbines are found as main exergy destruction components with 60.29%, 13.8%, 8.08%, and 6.66% , respectively. Besides, pumps, deaerator, and condenser components show the lowest exergy destruction.

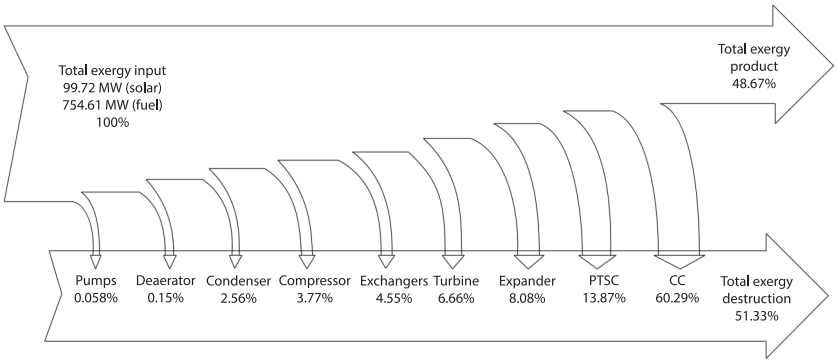

Figure 5. Exergy flow distribution of ISCCS

Advanced exergetic analysis results

To improve the accuracy of exergy analysis with a thorough understanding of thermodynamic inefficiencies, the exergy destruction is divided into avoidable, unavoidable, endogenous, and exogenous as shown in tab. 5. The exergy destruction rate of ISCCS components is shown in fig. 6. This approach facilitates the optimization and evaluation of each component of the system. Plainly, the advanced exergy analysis of the components results in 82.1% and

17.9% for endogenous exergy destruction rate (320.83 4MW) and exogenous exergy destruction rate (69.97 MW) , respectively. It indicating that the overall system's exergy destruction is mainly caused by the structure of the proposed ISCCS, while the exergy destruction caused by the interaction between various component units of the system is relatively small. Herein, the highest endogenous exergy destruction rate of 213.87 MW results in the combustion chamber followed by the PTSC's endogenous exergy destruction rate of 52.79 MW. Additionally, the exogenous exergy destruction of k^{th} component can be reduced by improving the reliability of other components in the system. While the endogenous exergy destruction of k^{th} component can be reduced by improving the technical level and the equipment structure. For example, the inevitable energy loss of the compressor can be reduced by interstage cooling and the efficiency of turbines can be improved by reheating the exhaust gas or steam.

Table 5. Results of the advanced exergy analysis of components

Component, k	$\dot{E}_{D,k}$ [MW]	$\dot{E}_{D,k}^{EN}$ [MW]	$\dot{E}_{D,k}^{EX}$ [MW]	$\dot{E}_{D,k}^{UN}$ [MW]	$\dot{E}_{D,k}^{AV}$ [MW]
Compressor	14.738	0.940	13.798	3.197	11.541
CC	235.634	213.870	21.764	213.870	21.764
Expander	31.592	19.991	11.602	24.098	7.494
Reheater	1.729	1.527	0.202	1.764	**–0.035**
HPSH	3.254	2.936	0.318	3.039	0.215
HPEVAP	3.473	2.931	0.541	3.031	0.442
HPECON	0.865	0.618	0.246	0.714	0.150
IPSH	0.299	0.197	0.102	0.297	0.002
IPEVAP	0.913	0.764	0.149	0.860	0.053
IPECON	1.148	0.823	0.325	0.913	0.235
LPSH	0.387	0.247	0.140	0.358	0.029
LPEVAP	1.260	0.863	0.397	0.953	0.307
Preheater	4.457	3.981	0.477	4.097	0.361
HPST	2.159	0.126	2.032	0.404	1.755
IPST	11.864	7.720	4.143	8.373	3.491
LPST	12.009	0.795	11.213	1.668	10.341
HP Pump	0.157	0.0003	0.156	0.011	0.146
IP Pump	0.052	0.0001	0.052	0.004	0.049
LP Pump	0.000	0.0000	0.000	0.000	0.000
Condensate Pump	0.017	0.0004	0.017	0.001	0.016
Condenser	10.003	9.041	0.961	9.046	0.957
Deaerator	0.590	0.665	**–0.075**	0.664	**–0.074**
PTSC	54.207	52.797	1.410	52.790	1.417
SUM	390.805	320.834	69.971	330.150	60.654

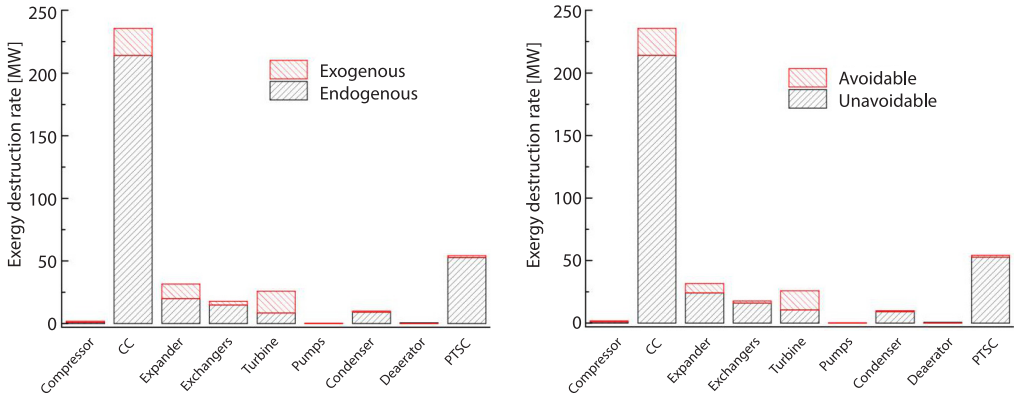

Figure 6. Exergy destruction rate of ISCCS components

Furthermore, the unavoidable exergy destructions of each component are calculated based on the unavoidable conditions, as demonstrated in tab. 2. The simulated results reveal the total unavoidable and avoidable exergy destruction rates of 330.15 MW and 60.65 MW, respectively. The combustion chamber, PTSC, and expander to unavoidable exergy destruction rates of 213.87 MW, 52.79 MW, and 24.01 MW. The highest exergy destruction rate of the combustion chamber is not only attributed to the large temperature difference between fuel and exhaust gas but also the irreversible combustion process. There is no doubt that most of the exergy destruction from the system is caused by structural factors in the component itself while the external system structure has less effect on operation status or exergy destruction. The reduced air-fuel ratio and preheated fuel can decrease the exergy destruction rate in the combustion chamber.

The second-largest exergy destruction rate is in the PTSC due to various exergy losses during the process of water heating into steam via solar energy and low temperature heat addition in the whole cycle. The high temperature of feed water supplied to PTSC and novel materials can reduce the exergy destruction. In the simulation, the positive or negative values of exergy destruction rates are resulted due to differences in flow rates between comparative conditions of interacted components. The efficiency of the components is improved due to the reduced exergy destruction rate under ideal and inevitable conditions.

Conclusions

The conventional and advanced exergetic analysis methods are adopted to investigate the exergy destruction of selected components in ISCCS. The energy-saving potential of components is calculated by the advanced exergetic analysis. The main conclusions are as followed:

The solar and chemical exergy are 99.72 MW and 754.61 MW for the ISCCS. For the overall system, a number of 48.67% of total exergy is converted to electricity with 51.33% loss. Additionally, for the components, the combustion chamber has the largest fuel exergy and the highest endogenous exergy destruction rate of 1001.60 MW and 213.87 MW, respectively. The combustion chamber has the highest exergy destruction rate of 235.60 MW (60.29%), followed by the PTSC of 54.20 MW (13.87%). For the overall system, the endogenous exergy destruction rate of 320.83 MW (82.10%) and the exogenous exergy destruction rate of 69.97 MW (17.90%) are resulted via the advanced exergy analysis method.

It is revealed that there are irreversible processes and a large amount of exergy destruction in the combustion chamber and PTSC. The structure of the system components and

integration method for ISCCS are considered feasible in order to improve the thermal performance of the system. The addition of multi-stage compression, an inter-cooling process in the compressor, reduce the air-fuel ratio and preheat fuel before burning in the combustion chamber can be the promising factors for the reduced exergy destruction under optimized operating conditions. The significance of the applied exergetic analysis method to reduce exergy destruction and improve energy-saving in the ISCCS.

Acknowledgment

This study was financially supported by the Fundamental Research Funds for the Central Universities (2018QN035) and the Ph. D. research startup foundation of Northeast Electric Power University (BSJXM-2020209)

Nomenclature

DNI – direct normal irradiance, [Wm^{-2}]
$\dot{E}_{L,tot}$ – exergy loss in the system, [kJkg^{-1}]
$\dot{E}x$ – exergy of a stream, [kJkg^{-1}]
$\dot{E}x_{D,k}$ – exergy destruction of kth component, [kJkg^{-1}]
$\dot{E}x_{F,k}$ – fuel exergy of kth component, [kJkg^{-1}]
$\dot{E}x_{P,k}$ – product exergy of kth component, [kJkg^{-1}]
$\dot{E}x_{ph}$ – physical exergy, [kJkg^{-1}]
$\dot{E}x_{ch}$ – chemical exergy, [kJkg^{-1}]
$\dot{E}x_{D,k}^{AV}$ – avoidable exergy destruction of kth component, [kJkg^{-1}]
$\dot{E}x_{D,k}^{EN}$ – endogenous exergy destruction of kth component, [kJkg^{-1}]
$\dot{E}x_{D,k}^{EX}$ – exogenous exergy destruction of kth component, [kJkg^{-1}]
$\dot{E}x_{D,k}^{UN}$ – unavoidable exergy destruction of kth component, [kJkg^{-1}]
h_{in} – specific enthalpy entering the system, [kJkg^{-1}]
h_{out} – specific enthalpy leaving the system, [kJkg^{-1}]
LHV – lower heating value, [kJkg^{-1}]
$\dot{m}$ – mass-flow, [kJs^{-1}]
Q_i – energy received by the collector, [kJ]
Q_L – energy loss, kJ
Q_s – energy absorbed by the absorbers, [kJ]
T_a – ambient temperature, [°C]
$y_{D,k}$ – exergy destruction rate, [%]

Greek symbol

η_{th} – mechanical efficiency
η_α – receiver absorption of collector
η_γ – acquisition factor of collector
η_μ – radiation and convective heat loss efficiency of the collector
η_ρ – surface reflectivity of collector
η_τ – receiver transmissivity of collector
η_ϕ – mirror utilization of collector

Acronyms

AC – air compressor
CC – combustion chamber
CCPP – combined cycle power plant
CPH – condensate preheater
CPC – compound parabolic concentrator
GT – gas turbine
Gen – generator
HEC – high-pressure economizer
HEV – high-pressure evaporator
HP – high pressure
HS – high-pressure superheater
HRSG – heat recovery steam generator
IEC – intermediate pressure economizer
IEV – intermediate pressure evaporator
IP – intermediate pressure
ISH – intermediate pressure superheater
ISCCS – integrated solar combined cycle power plant
LEV – low-pressure evaporator
LP – low pressure
LSH – low-pressure superheater
POEC– peak optical efficiency of collector
PTCS – parabolic trough solar collector
REH – rehaeter

Appendix A. Calculated thermodynamic variables for selected material streams

Stream, j	T_j [°C]	P_j [bar]	m_j [kgs^{-1}]	e_j [kJkg^{-1}]	h_j [kJkg^{-1}]	E_j [MW]
1	20.0	1.00	636.40	0.00	20.29	0.00
2	407.5	17.00	636.40	388.18	423.40	247.03
3	50.0	17.00	14.52	51955.9	109.05	754.61
4	1247.5	17.00	650.92	1176.80	1477.61	766.01
5	590.4	1.04	650.92	322.00	654.88	209.60
6	90.9	1.01	650.92	23.32	96.07	15.18
7	495.6	1.03	650.92	247.78	543.74	161.29
8	445.5	1.03	650.92	211.16	486.11	137.45
9	335.5	1.03	650.92	137.92	361.73	89.78
10	329.6	1.03	650.92	134.15	355.14	87.32
11	285.6	1.02	650.92	108.24	306.50	70.45
12	281.7	1.02	650.92	105.87	302.16	68.91
13	240.6	1.02	650.92	83.68	257.07	54.47
14	197.8	1.02	650.92	62.83	210.54	40.90
15	156.1	1.02	650.92	45.05	165.68	29.32
16	32.9	0.05	125.34	247.92	2375.07	31.07
17	32.9	0.05	125.34	7.58	137.76	0.95
18	32.9	4.70	125.34	8.06	138.35	1.01
19	119.0	4.65	125.34	85.37	499.87	10.70
20	149.1	4.65	199.52	127.67	628.46	25.47
21	149.1	4.70	199.52	127.68	628.47	25.47
22	149.1	4.65	199.52	179.24	774.48	35.76
23	149.1	4.65	13.80	875.06	2744.86	12.07
24	243.6	4.60	13.80	958.61	2949.36	13.23
25	149.1	4.65	83.87	127.67	628.46	10.71
26	149.6	29.90	83.87	130.66	631.90	10.96
27	230.6	29.85	83.87	278.83	992.97	23.39
28	233.6	29.85	199.52	352.66	1153.83	70.36
29	233.6	29.90	199.52	285.01	1007.07	56.87
30	233.6	29.85	16.22	1112.97	2803.26	18.05
31	329.5	29.80	16.22	1245.98	3067.68	20.20
32	230.6	29.85	67.66	278.53	992.97	18.85
33	233.3	126.10	67.66	291.47	1007.47	19.72
34	322.6	126.05	67.66	527.99	1475.47	35.72
35	328.5	126.10	70.50	549.85	1515.68	38.76
36	328.5	126.05	70.50	1176.82	2664.04	82.97
37	328.5	126.05	67.66	1181.22	2672.09	79.92
38	563.3	126.00	67.66	1688.43	3510.08	114.24
39	349.2	29.20	67.66	1270.33	3115.99	85.95
40	349.1	29.20	118.13	1270.14	3115.66	150.05
41	547.9	29.10	118.13	1548.17	3565.68	182.89
42	299.0	4.50	111.54	1012.82	3063.73	112.97
43	292.9	4.50	125.34	1006.27	3051.14	126.12
44	15.0	2.00	5209.85	1.77	63.17	9.20
45	27.9	1.50	5209.85	5.63	117.00	29.32
46	149.1	4.65	34.26	127.67	628.46	4.37
47	149.5	29.30	34.26	130.59	631.82	4.47
48	358.5	29.20	34.26	1282.58	3137.70	43.94
49	236.7	35.00	229.58	128.61	431.55	29.53
50	237.6	50.00	229.58	130.51	433.68	29.96
51	395.0	35.00	229.58	328.76	805.50	75.47

References

[1] Ghorbani, B., *et al.*, An Integrated Structure of Biomethane/Biomethanol Cogeneration Composed of Biogas Upgrading Process and Alkaline Electrolysis Unit Coupled with Parabolic trough Solar Collectors System, *Sustainable Energy Technologies and Assessments*, *46* (2021), 10134
[2] Malekan, M., *et al*., Heat Transfer Modelling of a Parabolic trough Solar Collector with Working Fluid of Fe_3O_4 and CuO/Therminol 66 Nanofluids under Magnetic Field, *Applied Thermal Engineering*, *163* (2019), 114435
[3] Ghazouani, M., *et al*., Thermal Energy Management Optimization of Solar Thermal Energy System Based on Small Parabolic trough Collectors for Bitumen Maintaining on Heat Process, *Solar Energy*, *211* (2020), Nov., pp. 1403-1421
[4] Jamel, M. S., *et al*., Shamsuddin A. H., Advances in the Integration of Solar Thermal Energy with Conventional and Non-Conventional Power Plants, *Renewable and Sustainable Energy Reviews*, *20* (2013), Apr., pp. 71-81
[5] Martín, J., *et al*., Thermoeconomic Evaluation of Integrated Solar Combined Cycle Systems (ISCCS), *Entropy*, *16* (2014), Sept., pp. 4246-4259
[6] Fallah, M., *et al*., Comparison of Different Gas Turbine Cycles and Advanced Exergy Analysis of the Most Effective, *Energy*, *116* (2016), Dec., pp. 701-715
[7] Yaghoubi, M., *et al*., Simulation of Shiraz Solar Power Plant for Optimal Assessment, *Renewable Energy*, *28* (2003), 12, pp. 1985-1998
[8] Adibhatla, S., *et al*., Energy, Exergy and Economic (3E) Analysis of Integrated Solar Direct Steam Generation Combined Cycle Power Plant, *Sustainable Energy Technologies and Assessments*, *20* (2017), Apr., pp. 88-97
[9] Baghernejad, A., *et al.*, Exergoeconomic Analysis and Optimization of an Integrated Solar Combined Cycle System (ISCCS) Using Genetic Algorithm, *Energy Conversion and Management*, *52* (2011), 5, pp. 2193-2203
[10] Petrakopoulou, F., *et al*., Conventional and Advanced Exergetic Analyses Applied to a Combined Cycle Power Plant, *Energy*, *41* (2012), 1, pp. 146-152
[11] Penkuhn, M., *et al*., Comparison of Different Ammonia Synthesis Loop Configurations with the Aid of Advanced Exergy Analysis, *Energy*, *137* (2017), Oct., pp. 854-864
[12] Galindo, J., *et al.*, Advanced Exergy Analysis for a Bottoming Organic Rankine Cycle Coupled to an Internal Combustion Engine, *Energy Conversion and Management*, *126* (2016), Oct., pp. 217-227
[13] Boyaghchi, F. A., *et al*., Advanced Exergy and Environmental Analyses and Multi Objective Optimization of a Real Combined Cycle Power Plant with Supplementary Firing Using Evolutionary Algorithm, *Energy*, *93* (2015), 2, pp. 2267-2279
[14] Fu, P., *et al*., Performance Degradation Diagnosis of Thermal Power Plants: A Method Based on Advanced Exergy Analysis, *Energy Conversion and Management*, *130* (2016), Dec., pp. 219-229
[15] Song, M., *et al*., Advanced Exergy Analysis for the Solid Oxide Fuel Cell System Combined with a Kinetic-Fuel Cell System Combined with a Kinetic-Based Modelling Pre-Reformer, *Energy Conversion and Management*, *245* (2021), 114560
[16] Yang, X. Q., *et al.*, Parametric Assessment, Multi-Objective Optimization and Advanced Exergy Analysis of a Combined Thermal-Compressed Air Energy Storage with an Ejector-Assisted Kalina Cycle, *Energy*, *239* (2022), 12148
[17] Li, L. Q., *et al*., Conventional and Advanced Exergy Analyses of a Vehicular Proton Exchange Membrane Fuel Cell Power System, *Energy*, *222* (2021), 119939
[18] Zhang, Y., *et al*., Advaned Exergy Analysis of an Integrated Energy Storage System Based on Transcritical CO_2 Energy Storage and Organic Rankine Cycle, *Energy Conversion and Management*, *216* (2020), 112938
[19] Wang, Y. L., *et al*., Advanced Exergy and Exergoeconomic Analysis of an Integrated System Combining CO_2 Capture-Storage and Waste Heat Utilization Processes, *Energy*, *219* (2021), 119600
[20] Jain, V., *et al*., Advanced Exergy Analysis and Risk Estimation of Novel NH_3-H_2O and H_2O-LiBr Integrated Vapor Absorption Refrigeration System, *Energy Conversion and Management*, *224* (2020), 113348
[21] Kaviri, A. G., *et al*., Modelling and Multi-Objective Exergy Based Optimization of a Combined Cycle Power Plant Using a Genetic Algorithm, *Energy Conversion and Management*, *58* (2012), June, pp. 94-103
[22] Anvari, S., *et al*., Employing a New Optimization Strategy Based on Advanced Exergy Concept for Improvement of a Tri-Generation System, *Applied Thermal Engineering*, *113* (2017), Feb., pp. 1452-1463
[23] Zhu, Y., *et al*., Exergy Destruction Analysis of Solar Tower Aided Coal-Fired Power Generation System Using Exergy and Advanced Exergetic Methods, *Applied Thermal Engineering, 108* (2016), Sept., pp. 339-346

[24] Xu, C., *et al*., Energy and Exergy Analysis of Solar Power Tower Plants, *Applied Thermal Engineering*, *31* (2011), 17-18, pp. 3904-3913
[25] Kaviri, A. G., *et al.*, Exergoenvironmental Optimization of Heat Recovery Steam Generators in Combined Cycle Power Plant through Energy and Exergy Analysis, *Energy Conversion and Management*, *67* (2013), Mar., pp. 27-33
[26] Bellos, E., *et al*., A Detailed Exergetic Analysis of Parabolic trough Collectors, *Energy Conversion and Management*, *149* (2017), Oct., pp. 275-292
[27] Muhammad ,S. K., *et al*., Numerical Performance Investigation of Parabolic Dish Solar-Assisted Cogeneration Plant Using Different Heat Transfer Fluids, *International Journal of Photoenergy*, *2021* (2021), ID5512679
[28] Akram, N., *et al*., Experimental Investigations of the Performance of a Flat-Plate Solar Collector Using Carbon and Metal Oxides Based Nanofluids, *Energy*, *227* (2021), 120452
[29] Liu, H., *et al.*, Thermodynamic Analysis of a Compressed Carbon Dioxide Energy Storage System Using Two Saline Aquifers at Different Depths as Storage Reservoirs, *Energy Conversion and Management*, *127* (2016), Nov., pp. 149-159
[30] Wang, L., *et al.*, Advanced Thermodynamic Analysis and Evaluation of a Supercritical Power Plant, *Energies*, *5* (2012), 12, pp. 1850-1863
[31] Balli, O., Advanced Exergy Analyses to Evaluate the Performance of a Military Aircraft Turbojet Engine (TJE) with Afterburner System: Splitting Exergy Destruction into Unavoidable/Avoidable and Endogenous/Exogenous, *Applied Thermal Engineering*, *111* (2017), Jan., pp. 152-169
[32] Salgado, C. L., *et al.*, Thermal Performance of Parabolic trough Solar Collectors, *Renewable and Sustainable Energy Reviews*, *67* (2017), Jan., pp. 1345-1359
[33] Morosuk, T., *et al.*, Comparative Evaluation of LNG – Based Cogeneration Systems Using Advanced Exergetic Analysis, *Energy*, *36* (2011), 6, pp. 3771-3778
[34] Penkuhn, M., *et al*., A Decomposition Method for the Evaluation of Component Interactions in Energy Conversion Systems for Application Advanced Exergy-Based Analyses, *Energy*, *133* (2017), Aug., pp. 388-403
[35] Mutani, G., *et al.*, An Urban Energy Atlas and Engineering Model for Resilient Cities, *International Journal of Heat and Technology*, *37* (2019), Dec., pp. 936-947
[36] Li, Y., *et al*., Impacts of Solar Multiples on the Performance of Integrated Solar Combined Cycle Systems with Two Direct Steam Generation Fields, *Applied Energy*, *160* (2015), Dec., pp. 637-680

Paper submitted: August 25, 2021
Paper revised: September 29, 2021
Paper accepted: October 18, 2021